

# Disruption of Chromodomain Helicase DNA Binding Protein 2 (*CHD2*) Causes Scoliosis

Shashikant Kulkarni,<sup>1</sup> Prabakaran Nagarajan,<sup>2</sup> Jonathan Wall,<sup>3</sup> Diana J. Donovan,<sup>1</sup> Robert L. Donell,<sup>4</sup> Azra H. Ligon,<sup>1</sup> Sundaresan Venkatachalam,<sup>2\*</sup> and Dr. Bradley J. Quade<sup>1\*\*</sup>

<sup>1</sup>Division of Women's and Perinatal Pathology and Clinical Cytogenetics Laboratory, Brigham and Women's Hospital and Department of Pathology, Harvard Medical School, Boston, Massachusetts

<sup>2</sup>Department of Biochemistry & Cellular and Molecular Biology, College of Veterinary Medicine, University of Tennessee, Knoxville, Tennessee

<sup>3</sup>Human Immunology and Cancer Program, Graduate School of Medicine, College of Veterinary Medicine, University of Tennessee, Knoxville, Tennessee

<sup>4</sup>Department of Pathobiology, College of Veterinary Medicine, University of Tennessee, Knoxville, Tennessee

Received 14 May 2007; Accepted 13 October 2007

Herein we characterize an apparently balanced de novo translocation, t(X;15)(p22.2;q26.1)dn, in a female patient with scoliosis, hirsutism, learning problems, and developmental delay (DGAP025). Other clinical findings include a high-arched palate, 2–3 syndactyly of the toes, and mildly elevated serum testosterone. No known or predicted genes are disrupted by the Xp22.2 breakpoint. The 15q26.1 breakpoint disrupts chromodomain helicase DNA binding protein 2 (*CHD2*). Another member of the chromatin-remodeling gene family, *CHD7*, has been associated with a defined constellation of congenital anomalies known as coloboma, heart anomaly, choanal atresia, mental retardation, genital and ear anomalies syndrome (CHARGE) and idiopathic scoliosis. Monosomy of 15q26 also has been associated with a spectrum of congenital abnormalities and growth retardation that overlaps with those of DGAP025. To

provide a biological correlate, we characterized a mutant mouse model with *Chd2* disruption that is associated with embryonic and perinatal lethality. Expression analysis indicated that *Chd2* is expressed in the heart, forebrain, extremities, facial and dorsal regions during specific times of embryonic development. *Chd2*<sup>+/m</sup> mice showed pronounced lordokyphosis, reduced body fat, postnatal runting, and growth retardation. These data suggest that haploinsufficiency for *CHD2* could result in a complex of abnormal human phenotypes that includes scoliosis and possibly features similar to CHARGE syndrome. © 2008 Wiley-Liss, Inc.

**Key words:** CHD2; chromodomain; helicase; congenital vertebral malformation; scoliosis; chromosomal translocation

**How to cite this article:** Kulkarni S, Nagarajan P, Wall J, Donovan DJ, Donell RL, Ligon AH, Venkatachalam S, Quade BJ. 2008. Disruption of chromodomain helicase DNA binding protein 2 (*CHD2*) causes scoliosis. *Am J Med Genet Part A* 146A:1117–1127.

## INTRODUCTION

Breakpoints analyzed in individuals with balanced chromosome rearrangements have led to the identification of various genes involved in human development [Ray et al., 1985; Blanquet et al., 1987; Turleau and de Grouchy, 1987; Ishikiriyama et al., 1989; Wallace et al., 1990; Zemni et al., 2000]. Identifying genes crucial in development through characterization of chromosomal rearrangements is the approach ongoing in the *Developmental Genome Anatomy Project* (DGAP; <http://dgap.harvard.edu>). Here we report our analysis of a 17-year-old Caucasian female (DGAP025) with multiple congenital abnormalities and t(X;15)(p22.2;q26.1)dn. Using high resolution FISH, we mapped the breakpoint on chromosome 15 within chromodomain

Shashikant Kulkarni and Prabakaran Nagarajan are contributed equally to this work.

Grant sponsor: National Institutes of Health; Grant numbers: T32 HL007627, GM061354; Grant sponsor: University of Tennessee seed funds.

Shashikant Kulkarni's present address is Division of Genetics and Genomic Medicine, Department of Pediatrics, Washington University Medical School at St. Louis, St. Louis, MO.

Prabakaran Nagarajan's present address is Department of Molecular and Cellular Biochemistry, The Ohio State University, Columbus, OH.

\*Correspondence to: Sundaresan Venkatachalam, Ph.D., Biochemistry & Cell and Molecular Biology, M407, Walters Life Sciences Building, University of Tennessee, Knoxville, TN 37996-6306.

E-mail: [sundar@utk.edu](mailto:sundar@utk.edu)

\*\*Correspondence to: Dr. Bradley J. Quade, M.D., Ph.D., Division of Women's and Perinatal Pathology, Brigham and Women's Hospital, 75 Francis Street, Boston, MA. E-mail: [bquade@partners.org](mailto:bquade@partners.org)

DOI 10.1002/ajmg.a.32178

helicase DNA binding protein 2 (*CHD2*), a member of the *CHD* family of genes. Mice in which a retroviral gene-trapping methodology truncates the murine ortholog within the DNA binding domain previously have been characterized to have growth and perinatal lethality in homozygous mutants, and glomerulopathy, other visceral organ pathology, and reduced survival in heterozygous mice [Marfella et al., 2006, 2007]. We independently characterized the same mouse model with a particular focus on skeletal analysis. In addition to finding embryonic lethality at E14.5 in homozygous mutants, we found runting, prominent vertebral anomalies and, occasionally, defective ocular development in heterozygous animals.

Chromodomain helicase DNA binding proteins were characterized as a distinct family of proteins in the late 1990s [Woodage et al., 1997]. *CHD* genes are evolutionarily conserved, and at least nine genes have been identified in humans ([Delmas et al., 1993; Woodage et al., 1997; Schuster and Stoger, 2002] and NCBI Build 36.2 ([http://www.ncbi.nlm.nih.gov/mapview/map\\_search.cgi?taxid=9606](http://www.ncbi.nlm.nih.gov/mapview/map_search.cgi?taxid=9606))). The *CHD* gene family is defined by the presence of chromo (*chromatin organization modifier*) domains, an SNF2-related helicase/ATPase domain and distinct DNA binding domains [Woodage et al., 1997]. Chromodomain containing proteins can self-associate as well as interact with the heterochromatic regions at centromeres, telomeres, and polytene chromosomes [Delmas et al., 1993; Schuster and Stoger, 2002]. CHD proteins modulate transcription by virtue of their ability to remodel chromatin structure via their helicase activities and effect on histone deacetylation [Singh et al., 1991; Cowell and Austin, 1997]. A wealth of data on the CHD family of proteins has come from studies showing CHD3 and CHD4 to be ATPases involved in chromatin remodeling [Cowell and Austin, 1997; Tong et al., 1998; Zhang et al., 1998; Brehm et al., 2000; Bowen et al., 2004]. The CHD3 and CHD4 proteins were also isolated as components of the nucleosome remodeling and histone deacetylation complex (NuRD) in HeLa cells [Targoff and Reichlin, 1985; Bowen et al., 2004]. The biological role of CHD2 is unknown. The chromosomal location of human *CHD2* is 15q26.1, a region implicated in a rare genetic disorder that leads to growth retardation, cardiac defects, and early post-natal lethality [Wilson et al., 1985; Whiteford et al., 2000].

Recently, mutations and microdeletions in *CHD7*, a *CHD* family member, have been shown in more than 60% of cases of CHARGE syndrome (OMIM 214800), a complex and nonrandom constellation of multiple congenital anomalies including Coloboma, Heart defects, choanal Atresia, mental Retardation, Genital and Ear anomalies [Vissers et al., 2004; Jongmans et al., 2006; Lalani et al., 2006]. In addition, linkage

analysis of familial idiopathic scoliosis has implicated *CHD7*, but the pathogenetic mutation(s) remain to be determined in the affected kindreds [Gao et al., 2007].

The association of scoliosis and other phenotypic problems with the disruption of *CHD2* in our human patient, as well as the targeted disruption of its murine ortholog, suggests that this member of the *CHD* gene family also plays a significant role in development and growth of the spine.

## MATERIALS AND METHODS

### Human Cell Line and Clinical Information

A lymphoblastoid cell line (NIGMS GM13992), established by Epstein–Barr virus transformation of peripheral blood lymphocytes from the patient (DGAP025), was obtained from the NIGMS Human Genetic Cell Repository at the Coriell Cell Repositories (Coriell Institute for Medical Research, Camden, NJ). The clinical information for this patient was acquired by the Repository when the original blood sample was submitted. We attempted to obtain additional detailed clinical description and follow-up information with the assistance of the Repository, but were unsuccessful due to the long interval between its original submission and our subsequent studies.

### Chromosome Preparations

Metaphase chromosomes were prepared using standard protocols. These chromosome spreads were used for GTG-banding, X-inactivation studies, and fluorescence in situ hybridization (FISH) [Ney et al., 1993]. FISH mapping of the chromosome breakpoints was carried out using bacterial artificial chromosome (BAC) and fosmid clones mapping to human chromosomes X and 15 (BACPAC Resource, CHORI, Oakland, CA) using methods previously described [Moore et al., 2004]. Clones were selected with the aid of the University of California Santa Cruz (UCSC) Genome Browser (May 2004 build; <http://genome.ucsc.edu/cgi-bin/hggateway>). BAC and fosmid DNA were prepared by strand displacement amplification using Phi29 DNA polymerase (GenomiPhi, GE Healthcare, Piscataway, NJ). DNA was directly labeled by nick translation using SpectrumGreen-dUTP or SpectrumRed-dUTP (Abbott Molecular/Vysis, Downers Grove, IL) and hybridized to metaphase chromosomes. Chromosomes were counterstained with 4', 6-diamidino-2-phenylindole (DAPI) and at least 10 metaphases per probe were analyzed using a CytoVision/Olympus BX51 microscopy system (Applied Imaging, San Jose, CA and Optical Analysis Corp., Nashua, NH).

### X-Inactivation Analysis

To assess the pattern of X-inactivation in DGAP025 lymphoblastoid cells, 5-bromo-2'-deoxyuridine (BrdU) replication timing studies were performed using standard protocols. Briefly, lymphoblastoid cells were grown in medium containing thymidine (0.3 mg/ml) and exposed to 30  $\mu$ g/ml BrdU (Sigma, St. Louis, MO) for 6 hr prior to harvesting. Metaphases were denatured and dehydrated. Incorporated BrdU was then detected using fluorescein isothiocyanate (FITC)-conjugated mouse monoclonal anti-BrdU antibody (Research Diagnostics, Flanders, NJ) according to the manufacturer's directions; a chromosome 15 fosmid clone was used to differentiate between the normal and derivative X chromosomes.

### Generation of *Chd2* Mutant Mice

We generated *Chd2*-deficient mice using the BayGenomics genetrap embryonic stem cell (ES) cell resource [Stryke et al., 2003]. *Chd2* trapped ES cells were obtained from BayGenomics and analyzed by PCR to confirm *Chd2* disruption using primers specific for *Chd2* and the gene-trap sequences. The following primers were used for genotype analysis of mutant and wild type mice: TR3, 5'-GTG AGC GAG TAA CAA CCC GTC-3'; TR2, 5'-AGC TGT TGG GAG GGT CAC TTT ATG-3'; TR1, 5'-ACC TGG CTC CTA TGG GAT AG-3'; GSP1, 5'-TGT GTG TCA GCA ATG CAG GA -3'; GSP2, 5'-TGC ATA ACC ATT CCG GGT GTG-3'. Sequencing of the PCR product indicated that the gene trap was integrated within intron 27 (1,563 base pairs from the beginning of the intron) of *Chd2*. Blastocyst injections from the validated ES cells were performed using the microinjection services at the University of Massachusetts Medical School, Worcester, MA. Resulting chimeras were bred to C57BL6/J mice to obtain founder *Chd2*<sup>+/-m</sup> mice (henceforth designated as *Chd2*<sup>+/-m</sup>). These heterozygotes were then intercrossed to yield 22 litters of 109 pups at F2 for phenotype analysis. Genotyping of the *Chd2*<sup>m</sup> allele was performed by Southern blot assays (data not shown) and PCR using the primers described above.

### Expression Analysis of *Chd2* During Mouse Development

Embryos obtained from timed matings from wild-type females and *Chd2*<sup>+/-m</sup> males were fixed with 1% paraformaldehyde and stained in a solution (2 mM MgCl<sub>2</sub>, 0.01% sodium deoxycholate, 0.02% NP-40, 5 mM potassium ferricyanide, 5 mM potassium ferrocyanide, 0.1 M phosphate buffer, pH 7.3) containing 5-bromo-4-chloro-3-indolyl-beta-D-galactopyranoside (X-gal). Genotypes of embryos were determined from genomic DNA isolated from yolk sacs.

### Imaging and 3D Reconstruction of Mutant Mice

High-resolution CT (Computed Tomography) images were acquired with a MicroCAT<sup>TM</sup> II (Siemens Medical Solutions Molecular Imaging, LLC, Knoxville, TN) instrument [Paulus et al., 2000; Wall et al., 2006]. The scanner is equipped with a 20–80 kVp microfocus X-ray source and has a 90 mm  $\times$  60 mm field of view. Each CT dataset was composed of 360 1-degree projections acquired over 8 min using a 310 msec exposure for each. Images were reconstructed using a modified version of the Feldkamp algorithm [Gregor et al., 2002] on a 512  $\times$  512  $\times$  768 matrix with an isotropic voxel size of 77  $\mu$ m. Micro CT data were visualized using the Amira 3-D image analysis software package (Amira, Version 3.1: Mercury Computer Systems, Chelmsford, MA).

## RESULTS

### Karyotypic and Phenotypic Description of DGAP025

DGAP025 is a 17-year-old Hispanic Caucasian female who presented with scoliosis, developmental delay, high arched palate, 2–3 syndactyly of the toes, learning problems, height < 30th centile and occipital frontal circumference (OFC) < 25th centile (Table D). In addition, the patient has a masculinized face, hirsutism, and excessive hair on her extremities. Her voice was characterized as low and somewhat masculine, her thorax shows secondary sexual development, her serum testosterone was 59 ng/dl (normal range for females: 10–55 ng/dl). Information allowing assignment to a specific Tanner Stage was not available. Her face (including the eyes and ears) was otherwise unremarkable (inner canthal distance, 3 cm; palpebral fissure distance, 2.5 cm; and ears, 6 cm).

The NIGMS Human Genetic Cell Repository karyotype, 46,X,t(X;15)(p22;q26.1)dn, for DGAP025 was confirmed prior to any FISH-mapping studies. The ideogram depicting the normal and derivative chromosomes X and 15 is shown in Figure 1A.

### X-Inactivation Analysis

The X-inactivation pattern was determined using an EBV-transformed lymphoblastoid cell line. The der(X) was identified using simultaneous FISH with a chromosome 15 fosmid clone. Results confirmed the expected inactivation pattern, in which the normal X was late replicating, in each of 50 metaphases analyzed (data not shown). This result indicates that the normal X was inactivated and that the etiology of this subject's phenotype was not subsequent to allelic imbalance due to inappropriate inactivation of autosomal DNA on the der(X) or lack of inactivation of X chromosomal DNA on the der(15).

TABLE I. Phenotypic Features Associated With Abnormalities of 15q26

Patient	Karyotype	Congenital anomalies <sup>a</sup>
DGAP025	46,X,t(X;15)(p22.2;q26.1)	<b>High arched palate, head circumference (25%), growth retardation</b> , learning problems, <b>scoliosis, 2–3 syndactyly of toes</b>
Klaassens et al. [2005]; 5 patients	46,XY,t(1;14),inv(6),del(15)(q26) 46,XY,r(15)(p11q26)	Genital anomalies, CDH, <b>IUGR</b> <b>Dysmorphic features</b> , cardiac, renal, genital and <b>limb abnormalities</b> , <b>IUGR</b> , CDH
Schlembach et al. [2001]	46,XY,r(15)(p11q26) 46,XX,r(15)(p11q26.3) 46,XY,del(15)(q26) 46,XX,del(15)(q25q26.2)	<b>Dysmorphic features</b> , cardiac abnormalities, <b>IUGR</b> , CDH Mental retardation, CDH, <b>mild dysmorphic features</b> , <b>IUGR</b> Mental retardation <b>Facial dysmorphism, short hands and feet, clino-/brachydactyly, digital contractures, rocker bottom feet</b> , renal hypoplasia, <b>IUGR</b>
Chen et al. [1998]	46,XX,der(15)t(8;15)(q24.1;q26.1)	<b>Craniofacial dysmorphism, kyphoscoliosis, clino-/campodactyly, overlapping of toes</b> , hydrocephalus, horseshoe kidney, ventricular septal defect, <b>IUGR</b>
Rosenberg et al. [1992]	46,XX,der(15)t(3;15)(q29;q26.1)	<b>Craniofacial dysmorphism</b> , heart malformation, single umbilical artery, <b>limb abnormalities</b> , <b>IUGR</b>
de Jong et al. [1989]	46,XY,r(15)(p11q26.1)	<b>Craniofacial dysmorphism, brachydactyly, limb abnormalities</b> , rocker bottom feet, small dysplastic kidneys, <b>IUGR</b>

CDH, congenital diaphragmatic hernia; IUGR, intra-uterine growth retardation.

<sup>a</sup>Overlapping phenotypic features are shown in bold type.

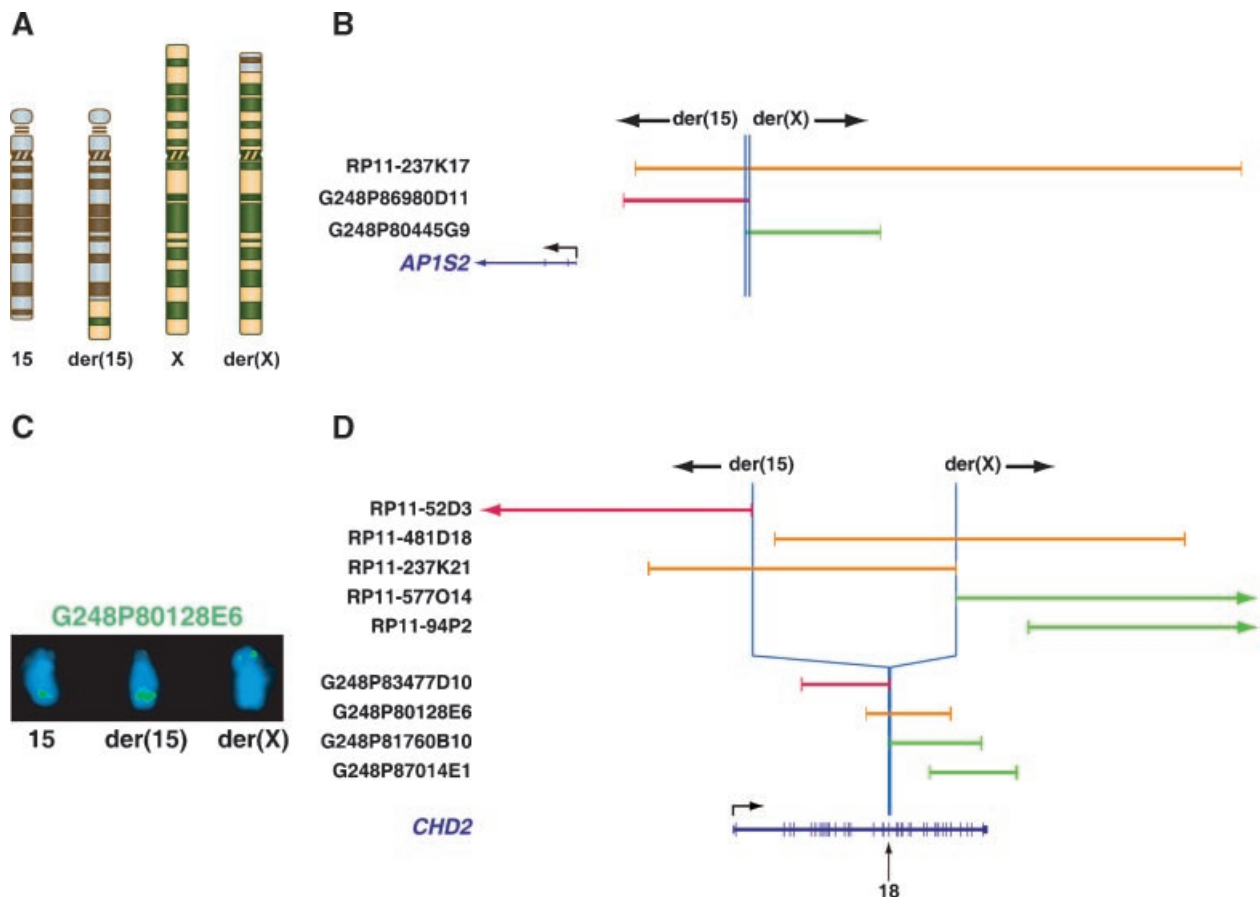


FIG. 1. Cytogenetic analysis of DGAP025. **A:** Ideogram illustrating the balanced t(X;15)(p22;q26.1)dn in DGAP025. Brown and blue shading, corresponding to GTG-positive and GTG-negative bands in metaphases, depicts chromosome 15 material in the two derivative chromosomes. Material from the X chromosome is shown similarly in green and yellow. **B:** Schematic representation of the Xp22 breakpoint region. BAC RP11-237K17 was split by the translocation. G248P86980D11 hybridized to the der(15) whereas G248P80445G9 hybridized to the der(X). Thus, the breakpoint mapped between two overlapping fosmids. The region overlapped by both clones, indicated by blue vertical lines, is 1.46 kb. The translocation disrupts no known or predicted genes. The gene nearest to the breakpoint (*AP1S2*) is about 16 kb telomeric to the breakpoint on the der(15). **C:** FISH with fosmid G248P80128E6. This partial metaphase shows hybridization signals (labeled in SpectrumGreen) on the der(15), der(X), and normal homolog of chromosome 15, indicating that this clone spans the 15p26.1 breakpoint. **D:** Schematic representation of the 15p26.1 breakpoint region. FISH performed with a series of overlapping BAC (upper) and fosmid (lower) clones to define the breakpoint region. Clones hybridizing only to the der(15) are indicated in red. Those hybridizing only to the der(X) are shown in green. Clones spanning the breakpoint are drawn in orange. The termini of clones correspond to short vertical lines in red, green or orange. Arrowheads denote clones terminating beyond the illustrated region.

### Breakpoint Mapping of the X Chromosome

To determine the site of breakage on the X chromosome, we performed FISH analysis with an ordered series of BAC and fosmid clones mapped to Xp22. The Xp22 breakpoint interval was narrowed to a region of about 1.46 kb using overlapping fosmid clones, G248P86980D11 and G248P80445G9 (Fig. 1B).

### Breakpoint Mapping of Chromosome 15

FISH performed with BAC clones RP11-52D3 and RP11-577O14 localized the breakpoint within an interval of ~98 kb. Further refinement of the chromosome 15 breakpoint using fosmids identified an ~416 bp interval within fosmid G248P80128E6 (Fig. 1C,D) flanked by fosmids G248P83477D10 and G248P81760B10. It also is possible that the breakpoint is located in one of the flanking fosmid clones because fluorescent signal generated by such a highly asymmetrically distributed FISH probe might be below the image capture system's detection threshold for one of the derivatives. In our experience, the breakpoint is usually with 10 kb of the clone's "flanking" end in such cases.

Only a single known gene, *CHD2*, maps within this interval, and the breakpoint region defined by FISH mapping localized it within intron 18 (Fig. 1D). Based on this FISH analysis, the chromosome 15 breakpoint was refined to 15q26.1.

### Expression of *Chd2* During Murine Development

To understand the relationship between the expression of chromodomain helicase DNA binding protein 2 and the abnormal phenotypes observed in

both DGAP025 and our mutant mouse model, we performed expression analysis using embryos obtained from timed matings between wild-type female mice and *Chd2* heterozygous males. The genetrap vector present in the *Chd2*-targeted ES cell clone contains a promoter-less  $\beta$ -galactosidase-neomycin fusion gene that allows expression analysis of the trapped *Chd2* gene (Fig. 2). The genotype of parents and offspring were determined by Southern blot analysis (not shown) and PCR (Fig. 2).

*Chd2* expression was limited to the para-aortic splanchnopleural mesoderm (P-Sp) region consisting of heart precursors in E10.5 embryos (Fig. 3A). At 10.5 d.p.c., expression was confined to the bulbus cordis and the common atrial chamber, predominantly areas that ultimately would develop into the right atrium and ventricle. One day later, new X-gal staining highlighted the forebrain and eye. Interestingly, strong X-gal staining appeared in the extremities, as well as the dorsal and facial regions in E15.5 embryos.

### Phenotypic Characterization of *Chd2* Mutant Mice

The germline disruption of genes with essential functions in embryogenesis usually leads to either embryonic lethality or developmental defects. Genotype analysis of tail DNA from offspring of F1 heterozygous intercrosses indicated that *Chd2* nullizygous mutants fail to survive. As shown in Table II, offspring from the 22 different F1 intercrosses did not yield any homozygous mutant offspring at weaning. These data also indicate that embryonic lethality is likely in a subset of heterozygous pups because the number of heterozygotes obtained was less than the

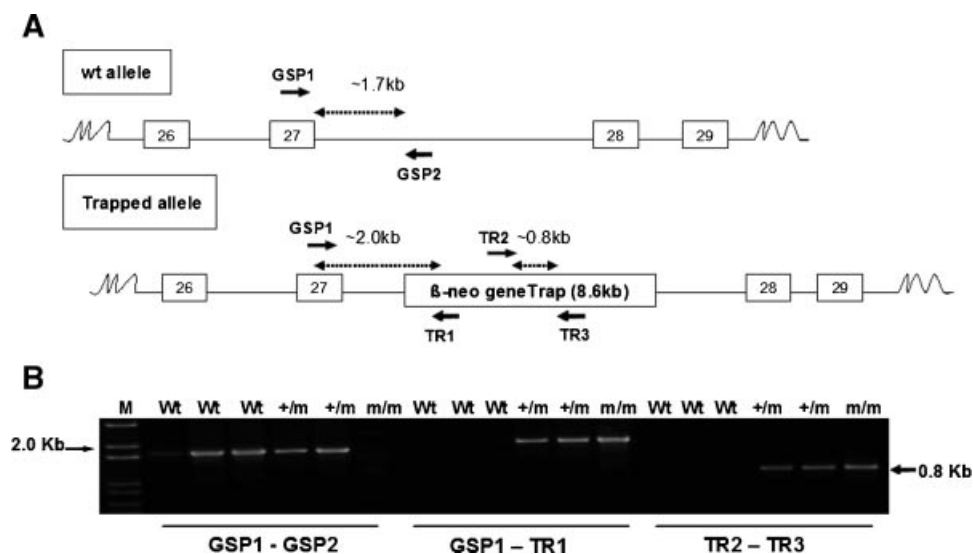


FIG. 2. **A:** Schematic representation of wild-type and trapped *Chd2* alleles. **B:** Genotype analysis of mutant and wild-type mouse embryonic fibroblasts are shown above. The relative positions of PCR primers used in the genotype analysis are indicated.

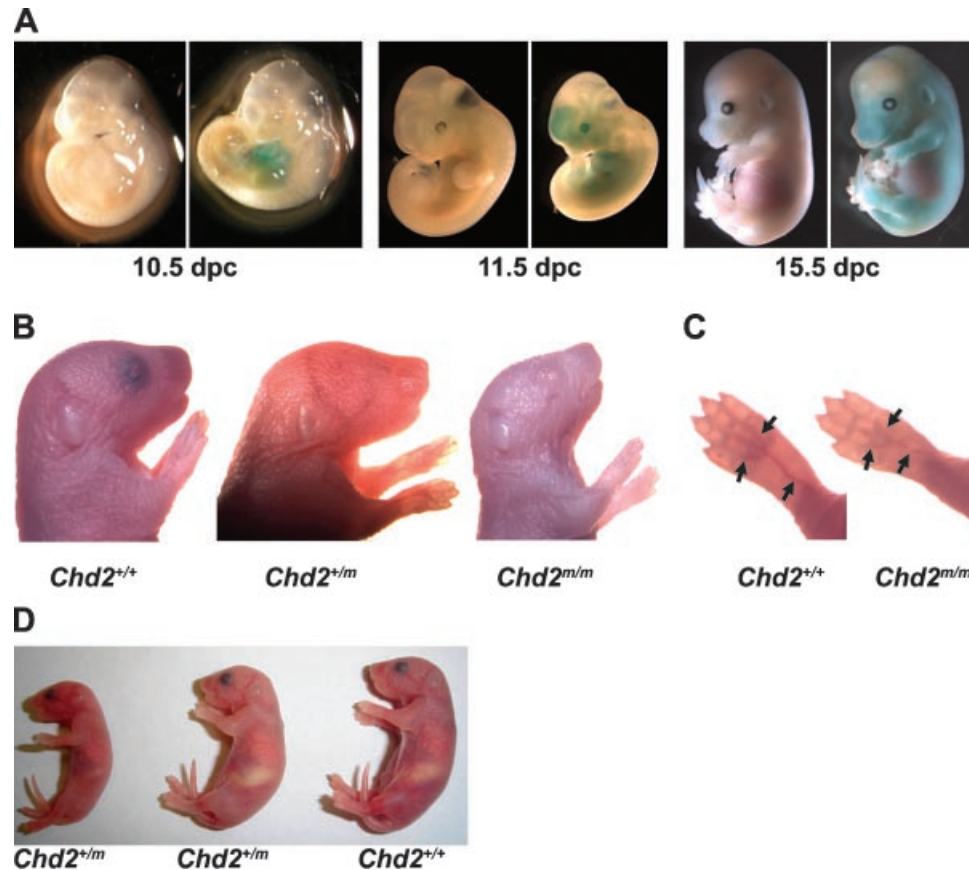


FIG. 3. Expression analysis of *Chd2* and phenotypic characterization of *Chd2*<sup>+/-</sup> and *Chd2*<sup>-/-</sup> mice. **A:** Expression analysis of *Chd2* during embryogenesis. Embryos at 10.5 (left), 11.5 (middle) and 15.5 d.p.c. (right) were stained with X-gal to assess  $\beta$ -galactosidase expression driven by the *Chd2* promoter. Wild-type (left, with no apparent X-gal staining) and heterozygote (right, stained blue) obtained from the same cross and treated similarly are shown. **B:** Lack of eye development was noted in some *Chd2*<sup>+/-</sup> and *Chd2*<sup>-/-</sup> embryos. **C:** Syndactyly, a finding in DGAP025, was not found in *Chd2*<sup>+/-</sup> and *Chd2*<sup>-/-</sup> mice. Filling defects in the vasculature of the distal extremities (arrows), however, were noted in some *Chd2*<sup>+/-</sup> mice. **D:** Growth retardation and reduced body fat were noted in *Chd2*<sup>+/-</sup> mice.

expected 2:1 ratio of the total offspring. To assess developmental defects that arise due to *Chd2* deficiency, we initiated timed matings and found that the lethality of the embryos began to occur around E14.5 as the number of null offspring was decreased at E14.5 (Table II). Neonatal mutants also appeared pale, runted and tended to wean later than their wild-type littermates. A small fraction (2/15 mutants) exhibited defective eye formation and eye migration defects (Fig. 3B). The adult heterozygous

offspring did not show any overt abnormalities except for apparent growth retardation. Most significantly, by 4 months, pronounced lordokyphosis was readily apparent (Fig. 4). In addition, the heterozygotes had a runt phenotype in which the subcutaneous fatty tissues were absent or extremely hypoplastic (Figs. 3D and 4D). Careful review of the distal extremities in heterozygous animals (n = 12) did not reveal any evidence of syndactyly or other gross digital abnormalities; filling defects in the distal vasculature, however, were noted and currently are under study (Fig. 2C). Finally, cystic endometrial hyperplasia was noted in three of eight female heterozygotes (data not shown). Unlike the murine phenotype described in a previous report [Marfella et al., 2006] we did not detect any cardiac anomaly apart from mild to moderate atrial enlargement in a subset of the *Chd2*<sup>+/-</sup> and *Chd2*<sup>-/-</sup> neonates (data not shown); nor were the stigmata of cardiac failure (*viz.*, hepatic centrilobular necrosis and hemosiderin-laden alveolar macrophages) present in the neonates. Renal histopathology also was not observed in the neonates, but ~47% (15/32) of adults

TABLE II. Embryonic and Neonatal Lethality of *Chd2* Mutant Mice\*

Developmental stage (# of intercrosses)	Total	<i>wt</i>	+/ <i>m</i> <sup>a</sup>	<i>m/m</i> <sup>a</sup>
E12.5 (n = 1)	7	1	3 (2)	3 (1)
E13.5 (n = 5)	44	8	25 (16)	11 (8)
E14.5 (n = 3)	15	5	8 (10)	2 (5)
Neonatal day 1 (n = 7)	58	16	34 (32)	8 (16)
Weanlings (n = 22)	109	56	53 (112)	0 (56)

\*The number of wild-type, heterozygous and homozygous mutants obtained at specific developmental stages and at weaning are shown.

<sup>a</sup>The expected number of mutants based on the observed number of wild-type offspring is given in parentheses.

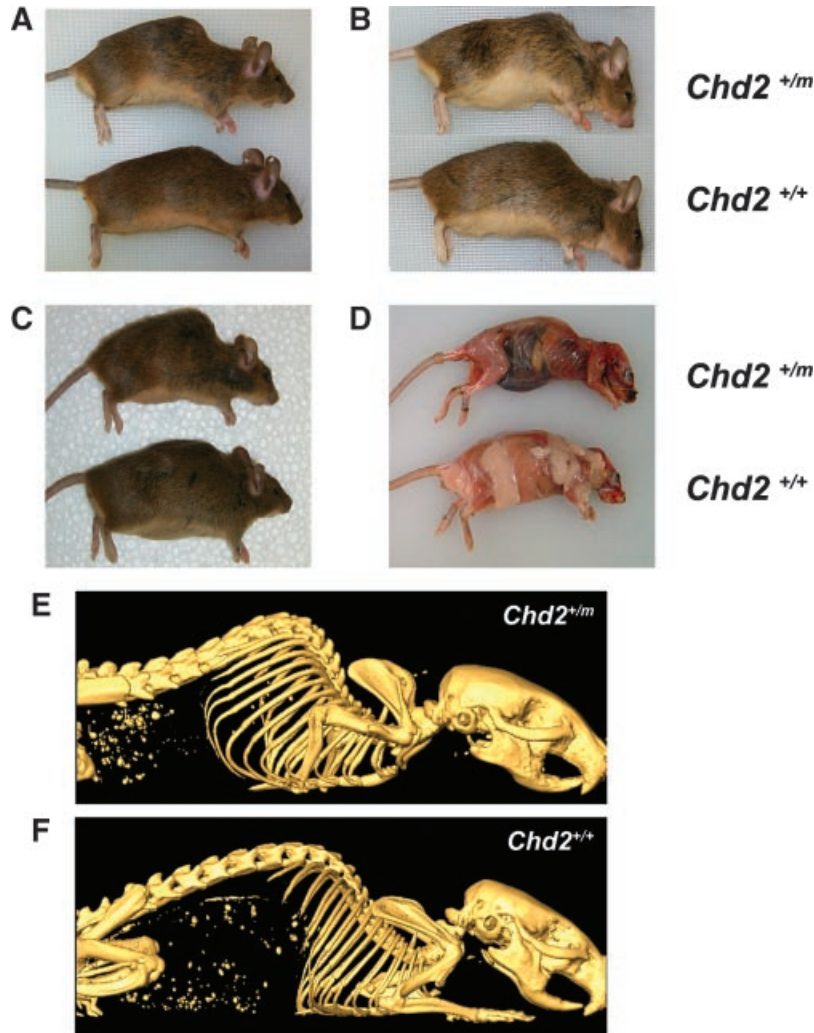


FIG. 4. *Chd2*<sup>+/m</sup> mice develop lordokyphosis as they age. **A:** 6 months, **(B)** 12 months, **(C)** 16 months, and **(D)** Skinned animals at 8 months. Note the markedly reduced body fat in the heterozygote. **E,F:** Computed-tomography reconstruction of the skeletal images of *Chd2*<sup>+/m</sup> and *Chd2*<sup>+/+</sup> mice at 15 months.

exhibited glomerulonephropathy (data not shown). The reasons for the phenotypic differences between mice characterized herein and those by Marfella et al. [2006] remain to be determined.

## DISCUSSION

We report on an X;autosome translocation, t(X;15)(p22.2;q26.1)dn, in a 17-year-old female with scoliosis, hirsutism, learning problems and developmental delay. Upon initial clinical examination, this particular constellation of malformations and developmental abnormalities did not correspond to any known syndrome.

Although we cannot completely exclude the possibility of disruption of an unannotated gene at Xp22.2, our results suggest that the chromosome 15 breakpoint is likely the pathogenetically relevant breakpoint. In addition, chromosome rearrangements as far as 1 Mb away from the transcription

and promotor region have been shown to affect gene expression [Velagaleti et al., 2005]. Accordingly, a position effect altering expression of a gene near the chromosome X breakpoint is possible, but data from other examples suggest that the distance is usually under 200 kb [Bedell et al., 1996; Kleinjan and van Heyningen, 1998, 2005]. Some of the genes in the vicinity of the chromosome X breakpoint and their respective distances relative to the breakpoint are *AP1S2*—16 kb, *U2AF1RS2*—48 kb, *CA5B*—86 kb, and *GRPR*—81 kb. The nearest of these, adaptor-related protein complex 1 (*AP1S2*,  $\sigma$ 2 subunit), localizes to the cytoplasmic face of coated vesicles of the Golgi complex, where it mediates clathrin recruitment [Takatsu et al., 1998]. *U2AF1RS2* (*U2AF1L2*, U2 small nuclear ribonucleoprotein auxiliary factor, small subunit 2), encodes a protein related to an essential splicing factor [Kitagawa et al., 1995]. *CA5B* (carbonic anhydrase VB, mitochondrial) is a member of the zinc metalloenzyme family that

catalyze the reversible hydration of carbon dioxide [Fujikawa-Adachi et al., 1999]. The most distant, *GRPR* (gastrin-releasing peptide receptor), regulates numerous functions of the gastrointestinal and central nervous systems, including release of gastrointestinal hormones, smooth muscle cell contraction, and epithelial cell proliferation [Spindel et al., 1990]. Of the genes near the X chromosome breakpoint, only *GRPR* has been implicated to play a role in human development. Specifically, an individual with autism, a phenotype unlike that of DGAP025, was found to have a balanced translocation between *GRPR* on Xp22.12 and 8q22.1 [Ishikawa-Brush et al., 1997].

In addition to DGAP025, at least eight other patients are reported in the literature with some overlapping phenotype and similar chromosomal breakpoints or deletions involving 15q25-26 (Table I) [de Jong et al., 1989; Rosenberg et al., 1992; Chen et al., 1998; Schlembach et al., 2001; Klaassens et al., 2005]. Six of these eight patients had craniofacial dysmorphism and limb abnormalities with 15q26 chromosomal breakpoints. The growth retardation in DGAP025 and in other cases reported in the literature (Table I) also is consistent with the location of a key developmental regulator gene at 15q26. The most interesting candidate gene in the region of overlapping deletion is the one directly disrupted by the chromosomal rearrangement in DGAP025, namely *CHD2* [Woodage et al., 1997].

Recently, causative mutations and deletions of *CHD7*, another CHD family member, have been identified in roughly 60% of individuals with CHARGE syndrome [Vissers et al., 2004; Lalani et al., 2006]. Expression analysis of murine embryos and neonates demonstrates increased *CHD7* expression in tissues corresponding to the adult structures affected in CHARGE syndrome [Bosman et al., 2005; Lalani et al., 2006; Sanlaville et al., 2006]. Multiple ENU-induced mutations in *Cbd7* result in a variety of partially or nearly fully truncated polypeptide products and a range of defects with reduced penetrance that include cleft palate, choanal atresia, cardiac septal defects, vulvar and clitoral defects, keratoconjunctivitis sicca, and perinatal death [Bosman et al., 2005]. In the human, *CHD7* polymorphisms have recently been associated a familial susceptibility to idiopathic scoliosis, particularly those manifesting during the accelerated growth of adolescence [Gao et al., 2007]. In contrast to the murine mutations, the mechanistic significance of the newly identified human *CHD7* polymorphisms remains to be elucidated. Finally, Gao et al. [2007] have suggested that *CHD7* may have been disrupted by position effect over 9.9 Mb in an individual with idiopathic scoliosis and pericentric chromosomal inversion between 8p23.2 and 8q11.21 [Bashiardes et al., 2004].

*CHD2* is a 38 exon, ~122 kb member of the CHD gene family. *CHD2*, like *CHD7*, is a protein with two chromatin organization modifier (chromo) domains, a SNF2-related helicase/ATPase domain and a DNA-binding domain [Woodage et al., 1997]. CHD proteins alter gene expression by modifying nucleosome binding and remodeling, which presumably modulates access of the transcriptional machinery to the DNA template.

Prior to this study, no association between *CHD2* defects and a human phenotype has yet been proven prior to this study, although *CHD2* recently was one of several genes within 15q26.1 implicated in congenital diaphragmatic hernia [Klaassens et al., 2005]. Specifically, monosomy 15q26.1–15q26.2 occurs recurrently in individuals with congenital diaphragmatic hernia [Slavotinek et al., 2006]. In the study by Slavotinek and co-authors, only one Mexican-American patient of more than 100 ethnically diverse individuals with congenital diaphragmatic hernia had a missense change (C5128T, corresponding to R1710W), which was not found in 100 ethnically matched normal controls [Slavotinek et al., 2006]. Of note, this particular sequence variation was not associated with any other phenotypic abnormalities and, consequently, C5128T was judged not to be pathogenetic for congenital diaphragmatic hernia. The lack of clinically evident diaphragmatic herniation in DGAP025 and our mutant mouse model is consistent with lack of a critical role for *CHD2* in development of the diaphragm, but raises the possibility that another gene in the critical deletion interval might be causative. Recently, it has been shown that mice lacking *NR2F2*, which maps to 15q26.2 approximately 3.3 Mb from *CHD2*, are born with Bochdalek-type congenital diaphragmatic hernias [You et al., 2005].

Disruption of *CHD2* could contribute to the phenotype in DGAP025 either through formation of a fusion product with a gene on the X chromosome or by *CHD2* truncation, causing haploinsufficiency or perhaps a dominant negative effect. In CHARGE syndrome associated with *CHD7* mutations, nearly three-quarters (47/64) of mutations in a single series were predicted to result in premature termination of the protein, which was interpreted as supporting the haploinsufficiency model [Lalani et al., 2006]. The genomic orientation of the genes surrounding the chromosomal breakpoints in DGAP025 is such that a 5'-*CHD2*-*APIS2*-3' fusion would be feasible if the transcription excluded the first exon of *APIS2* (exon jumping). The orientation of the other nearby genes would not support the formation of additional fusion products. Alternatively, the hypothetical truncation product would retain two chromo domains and the SNF2 domain, but omit the C-terminal helicase domain. Nonetheless, we searched for either a fusion transcript between the 5' of

*CHD2* and the 3' of a gene on the X chromosome or a truncated *CHD2* transcript using 3' RACE PCR experiments (data not shown) using the EBV-transformed lymphoblast cell line and found neither. The absence of such aberrant transcripts suggests that they may not contribute to the DGAP025 phenotype, although it is possible that such mRNA species were expressed either at different times or in different cell types during the development of DGAP025. In the mouse model, insertion of the retroviral gene-trap results in truncation of *Cbd2* in the DNA binding domain and, presumably, abrogation of the DNA binding domain's function [Marfella et al., 2007]. Although the extent of truncation differs between DGAP025 and the mouse model, the similarity in these mutations suggests that the mechanism responsible for the resulting phenotypes also may be shared. Consequently, our analysis of the t(X;15)(p22.2;q26.1)dn in DGAP025 supports the view that haploinsufficiency for *CHD2* is the most likely explanation for the observed phenotypic features.

Mutation of both *Cbd2* alleles in the mouse results in embryonic and perinatal lethality, clearly indicating that this chromodomain helicase DNA binding protein family member is important during development. Like *CHD7*, the pattern of embryonic expression (eye, heart, face, and forebrain) correlates with most of the affected organs and tissues defining the coloboma, heart anomaly, choanal atresia, retardation, genital and ear anomalies syndrome (CHARGE). The concurrence of cardiac *Cbd2* expression and embryonic lethality of *Cbd2* nullizygosity suggests that lethality may be due to a failure to achieve a critical milestone in cardio-vascular or hematopoietic development. Later in postnatal life, the most striking anomaly noted in *Cbd2* heterozygotes was marked lordokyphosis. *CHD2* disruption in the human (DGAP025) also was associated with clinically significant scoliosis. Of note, Doyle and Blake [Doyle and Blake, 2005] report that nearly two-thirds (19/31) of individuals with a clinical diagnosis of CHARGE syndrome have scoliosis that was moderate to severe in 40% (8/19) of cases. Interestingly, they suggest that CHARGE syndrome with scoliosis may represent a specific subtype because, on average, the diagnosis of CHARGE syndrome was delayed by over 2 years (6.3 years of age compared to 3.7 years of age) in cases without scoliosis. In addition, scoliosis was associated with growth hormone therapy. The location of the anomalous vertebral development and growth may correlate with the dorsal expression of *Cbd2* in the mouse embryo at 15.5 d.p.c. Although syndactyly was not observed in the mouse model, *Cbd2* expression was also prominent in growing limbs, and a mechanism similar to that responsible for the vertebral anomaly could be postulated for anomalous digital development in DGAP025.

Other phenotypic features in DGAP025, and possibly in those individuals with monosomy for regions of 15q (Table I), also can be correlated with the heterozygous mouse. Intrauterine growth retardation (IUGR) is a common characteristic of all previously reported patients with monosomy 15q26 (Table I and [Kristofferson et al., 1987; Formiga et al., 1988; Roback et al., 1991]). DGAP025 showed a decreased occipital-frontal circumference (OFC) and height, whereas the *Cbd2*<sup>+/*m*</sup> mouse showed a runt phenotype with reduced body fat. Reduced fetal growth might be attributable to dysregulation of a key regulator of early fetal development. Haploinsufficiency of insulin-like growth factor 1 receptor (*IGF1R*) has been proposed as a possible factor for growth retardation [Nagai et al., 2002]. *IGF1R*, however, is unlikely to be the responsible gene in DGAP025 as it maps telomeric to *CHD2* in 15q26.3. The relationship, if any, between the other phenotypic features of DGAP025 (*viz.*, stigmata of hyperandrogenism, high arched palate, and learning problems) and the embryonic murine pattern of expression (facial area and forebrain) remains to be determined. Of note, both DGAP025 and *Cbd2*<sup>+/*m*</sup> females show phenotypic features (hyperandrogenism and endometrial hyperplasia, respectively) that could be attributed to an abnormal anovulatory endocrinological state. Elevation of serum testosterone levels, however, could not be confirmed in *Cbd2*<sup>+/*m*</sup> female mice (data not shown). This potential difference in phenotypic expression between mice and human, however, may be a reflection of basic differences in their respective reproductive physiology. It is also possible that further investigation of *CHD2* in DGAP025 and our mouse model may expand the definition of CHARGE syndrome.

In conclusion, we mapped a developmentally critical *CHD* gene to 15q26.1 in the human, a region that has been implicated in multiple congenital anomalies, and we report similar features in a *Cbd2* mutant mouse model. Taken together with known disruptions and mutations in another chromatin remodeling gene family member (*CHD7*), these data suggest a potential role for *CHD2* in embryonic development, possibly through alteration of chromatin structure and subsequent gene expression. This first demonstration of *CHD2* mutation leading to abnormal development of the spine and other organs, in both man and mouse, provides the basis for future studies to explore further growth and development, as well as to study further the origins of the CHARGE syndrome. Identification of similar individuals with breakpoints, deletions, or mutations involving *CHD2* and phenotypes similar to those observed in DGAP025 and our mouse model will clarify further the contributions of *CHD2* and chromatin regulation to embryonic development.

## ACKNOWLEDGMENTS

We are indebted to Robert E. Eisenman for technical assistance and to Amy Bosco, Heather L. Ferguson, and Chantal Kelly for their expertise as genetic counselors for the Developmental Genome Anatomy Project. We are most grateful to Dr. Cynthia Morton for the helpful conversations during this project and for reviewing this manuscript. We would also like to thank kindly Dr. Jay C. Leonard of the NIGMS Cell Repository, Coriell Cell Repositories, Coriell Institute for Medical Research for his assistance with and support of the Developmental Genome Anatomy Project. The authors wish to acknowledge the following support of the research by the National Institutes of Health (T32 HL007627 to S.K.; GM061354 to A.H.L., and B.J.Q.) and University of Tennessee seed funds (to S.V.).

## REFERENCES

- Bashiardes S, Veile R, Allen M, Wise CA, Dobbs M, Morcuende JA, Szappanos L, Herring JA, Bowcock AM, Lovett M. 2004. *SNTG1*, the gene encoding gamma1-syntrophin: A candidate gene for idiopathic scoliosis. *Hum Genet* 115:81–89.
- Bedell MA, Jenkins NA, Copeland NG. 1996. Good genes in bad neighbourhoods. *Nat Genet* 12:229–232.
- Blanquet V, Turleau C, Creau-Goldberg N, Cochet C, de Grouchy J. 1987. *De novo* t(2;13)(p24.3;q14.2) and retinoblastoma. Mapping of two 13q14 probes by *in situ* hybridization. *Hum Genet* 76:102–105.
- Bosman EA, Penn AC, Ambrose JC, Kettleborough R, Stemple DL, Steel KP. 2005. Multiple mutations in mouse *Chd7* provide models for CHARGE syndrome. *Hum Mol Genet* 14:3463–3476.
- Bowen NJ, Fujita N, Kajita M, Wade PA. 2004. Mi-2/NuRD: Multiple complexes for many purposes. *Biochim Biophys Acta* 1677:52–57.
- Brehm A, Langst G, Kehle J, Clapier CR, Imhof A, Eberharder A, Muller J, Becker PB. 2000. dMi-2 and ISWI chromatin remodelling factors have distinct nucleosome binding and mobilization properties. *EMBO J* 19:4332–4341.
- Chen CP, Lee CC, Pan CW, Kir TY, Chen BF. 1998. Partial trisomy 8q and partial monosomy 15q associated with congenital hydrocephalus, diaphragmatic hernia, urinary tract anomalies, congenital heart defect and kyphoscoliosis. *Prenat Diagn* 18:1289–1293.
- Cowell IG, Austin CA. 1997. Self-association of chromo domain peptides. *Biochim Biophys Acta* 1337:198–206.
- de Jong G, Rossouw RA, Retief AE. 1989. Ring chromosome 15 in a patient with features of Fryns' syndrome. *J Med Genet* 26:469–470.
- Delmas V, Stokes DG, Perry RP. 1993. A mammalian DNA-binding protein that contains a chromodomain and an SNF2/SWI2-like helicase domain. *Proc Natl Acad Sci USA* 90:2414–2418.
- Doyle C, Blake K. 2005. Scoliosis in CHARGE: A prospective survey and two case reports. *Am J Med Genet Part A* 133A:340–343.
- Formiga LD, Poenaru L, Couronne F, Flori E, Eibel JL, Deminatti MM, Savary JB, Lai JL, Gilgenkrantz S, Pierson M. 1988. Interstitial deletion of chromosome 15: Two cases. *Hum Genet* 80:401–404.
- Fujikawa-Adachi K, Nishimori I, Taguchi T, Onishi S. 1999. Human mitochondrial carbonic anhydrase VB. cDNA cloning, mRNA expression, subcellular localization, and mapping to chromosome x. *J Biol Chem* 274:21228–21233.
- Gao X, Gordon D, Zhang D, Browne R, Helms C, Gillum J, Weber S, Devroy S, Swaney S, Dobbs M, Morcuende J, Sheffield V, Lovett M, Bowcock A, Herring J, Wise C. 2007. CHD7 gene polymorphisms are associated with susceptibility to idiopathic scoliosis. *Am J Hum Genet* 80:957–965.
- Gregor J, Gleason SS, Paulus MJ, Cates J. 2002. Fast Feldkamp reconstruction based on focus of attention and distributed computing. *Int J Imaging Systems Technol* 12:229–234.
- Ishikawa-Brush Y, Powell JF, Bolton P, Miller AP, Francis F, Willard HF, Lehrach H, Monaco AP. 1997. Autism and multiple exostoses associated with an X;8 translocation occurring within the *GRPR* gene and 3' to the *SDC2* gene. *Hum Mol Genet* 6:1241–1250.
- Ishikiriyama S, Tonoki H, Shibuya Y, Chin S, Harada N, Abe K, Niikawa N. 1989. Waardenburg syndrome type I in a child with *de novo* inversion (2)(q35q37.3). *Am J Hum Genet* 33:505–507.
- Jongmans MC, Admiraal RJ, van der Donk KP, Vissers LE, Baas AF, Kapusta L, van Hagen JM, Donnai D, de Ravel TJ, Veltman JA, Geurts van KA, De Vries BB, Brunner HG, Hoefsloot LH, van Ravenswaaij CM. 2006. CHARGE syndrome: The phenotypic spectrum of mutations in the *CHD7* gene. *J Med Genet* 43:306–314.
- Kitagawa K, Wang X, Hatada I, Yamaoka T, Nojima H, Inazawa J, Abe T, Mitsuya K, Oshimura M, Murata A. 1995. Isolation and mapping of human homologues of an imprinted mouse gene *U2af1-rs1*. *Genomics* 30:257–263.
- Klaassens M, van DM, Eussen HJ, Douben H, den Dekker AT, Lee C, Donahoe PK, Galjaard RJ, Goemaere N, de Krijger RR, Wouters C, Wauters J, Oostra BA, Tibboel D, de Klein A. 2005. Congenital diaphragmatic hernia and chromosome 15q26: Determination of a candidate region by use of fluorescent *in situ* hybridization and array-based comparative genomic hybridization. *Am J Hum Genet* 76:877–882.
- Kleinjan DJ, van Heyningen V. 1998. Position effect in human genetic disease. *Hum Mol Genet* 7:1611–1618.
- Kleinjan DA, van Heyningen V. 2005. Long-range control of gene expression: Emerging mechanisms and disruption in disease. *Am J Hum Genet* 76:8–32.
- Kristoffersson U, Heim S, Mandahl N, Sundkvist L, Szelest J, Hagerstrand I. 1987. Monosomy and trisomy of 15q24-pter in a family with a translocation t(6;15)(p25;q24). *Clin Genet* 32:169–171.
- Lalani SR, Safiullah AM, Fernbach SD, Harutyunyan KG, Thaller C, Peterson LE, McPherson JD, Gibbs RA, White LD, Hefner M, Davenport SL, Graham JM, Bacino CA, Glass NL, Towbin JA, Craigen WJ, Neish SR, Lin AE, Belmont JW. 2006. Spectrum of CHD7 mutations in 110 individuals with CHARGE syndrome and genotype-phenotype correlation. *Am J Hum Genet* 78:303–314.
- Marfella CG, Ohkawa Y, Coles AH, Garlick DS, Jones SN, Imbalzano AN. 2006. Mutation of the SNF2 family member *Chd2* affects mouse development and survival. *J Cell Physiol* 209:162–171.
- Marfella CG, Ohkawa Y, Coles AH, Garlick DS, Jones SN, Imbalzano AN. 2007. Mutation of the SNF2 family member *Chd2* affects mouse development and survival—Erratum. *J Cell Physiol* 212:562.
- Moore SD, Herrick SR, Ince TA, Kleinman MS, Cin PD, Morton CC, Quade BJ. 2004. Uterine leiomyomata with t(10;17) disrupt the histone acetyltransferase *MORF*. *Cancer Res* 64:5570–5577.
- Nagai T, Shimokawa O, Harada N, Sakazume S, Ohashi H, Matsumoto N, Obata K, Yoshino A, Murakami N, Murai T, Sakuta R, Niikawa N. 2002. Postnatal overgrowth by 15q-trisomy and intrauterine growth retardation by 15q-monosomy due to familial translocation t(13;15): Dosage effect of IGF1R? *Am J Med Genet* 113:173–177.
- Ney PA, Andrews NC, Jane SM, Safer B, Purucker ME, Wermowicz S, Morton CC, Goff SC, Orkin SH, Nienhuis AW. 1993. Purification of the human NF-E2 complex: cDNA cloning of

- the hematopoietic cell-specific subunit and evidence for an associated partner. *Mol Cell Biol* 13:5604–5612.
- Paulus MJ, Gleason SS, Kennel SJ, Hunsicker PR, Johnson DK. 2000. High resolution X-ray computed tomography: An emerging tool for small animal cancer research. *Neoplasia* 2: 62–70.
- Ray PN, Belfall B, Duff C, Logan C, Kean V, Thompson MW, Sylvester JE, Gorski JL, Schmickel RD, Worton RG. 1985. Cloning of the breakpoint of an X;21 translocation associated with Duchenne muscular dystrophy. *Nature* 318:672–675.
- Roback EW, Barakat AJ, Dev VG, Mbikay M, Chretien M, Butler MG. 1991. An infant with deletion of the distal long arm of chromosome 15 (q26.1-qter) and loss of insulin-like growth factor 1 receptor gene. *Am J Med Genet* 38:74–79.
- Rosenberg C, Blakemore KJ, Kearns WG, Giraldez RA, Escallon CS, Pearson PL, Stetten G. 1992. Analysis of reciprocal translocations by chromosome painting: Applications and limitations of the technique. *Am J Hum Genet* 50:700–705.
- Sanlaville D, Etchevers HC, Gonzales M, Martinovic J, Clement-Ziza M, Delezoide AL, Aubry MC, Pelet A, Chemouny S, Cruaud C, Audollent S, Esculpavit C, Goudefroye G, Ozilou C, Fredouille C, Joye N, Morichon-Delvallez N, Dumez Y, Weissenbach J, Munnich A, Amiel J, Encha-Razavi F, Lyonnet S, Vekemans M, Tite-Bitach T. 2006. Phenotypic spectrum of CHARGE syndrome in fetuses with *CHD7* truncating mutations correlates with expression during human development. *J Med Genet* 43:211–217.
- Schlembach D, Zenker M, Trautmann U, Ulmer R, Beinder E. 2001. Deletion 15q 24-26in prenatally detected diaphragmatic hernia: Increasing evidence of a candidate region for diaphragmatic development. *Prenat Diagn* 21:289–292.
- Schuster EF, Stoger R. 2002. CHD5 defines a new subfamily of chromodomain-SWI2/SNF2-like helicases. *Mamm Genome* 13:117–119.
- Singh PB, Miller JR, Pearce J, Kothary R, Burton RD, Paro R, James TC, Gaunt SJ. 1991. A sequence motif found in a Drosophila heterochromatin protein is conserved in animals and plants. *Nucleic Acids Res* 19:789–794.
- Slavotinek AM, Moshrefi A, Davis R, Leeth E, Schaeffer GB, Burchard GE, Shaw GM, James B, Ptacek L, Pennacchio LA. 2006. Array comparative genomic hybridization in patients with congenital diaphragmatic hernia: Mapping of four CDH-critical regions and sequencing of candidate genes at 15q26.1-15q26.2. *Eur J Hum Genet* 14:999–1008.
- Spindel ER, Giladi E, Brehm P, Goodman RH, Segerson TP. 1990. Cloning and functional characterization of a complementary DNA encoding the murine fibroblast bombesin/gastrin-releasing peptide receptor. *Mol Endocrinol* 4:1956–1963.
- Stryke D, Kawamoto M, Huang CC, Johns SJ, King LA, Harper CA, Meng EC, Lee RE, Yee A, L'Italien L, Chuang PT, Young SG, Skarnes WC, Babbitt PC, Ferrin TE. 2003. BayGenomics: A resource of insertional mutations in mouse embryonic stem cells. *Nucleic Acids Res* 31:278–281.
- Takatsu H, Sakurai M, Shin HW, Murakami K, Nakayama K. 1998. Identification and characterization of novel clathrin adaptor-related proteins. *J Biol Chem* 273:24693–24700.
- Targoff IN, Reichlin M. 1985. The association between Mi-2 antibodies and dermatomyositis. *Arthritis Rheum* 28:796–803.
- Tong JK, Hassig CA, Schnitzler GR, Kingston RE, Schreiber SL. 1998. Chromatin deacetylation by an ATP-dependent nucleosome remodeling complex. *Nature* 395:917–921.
- Turleau C, de Grouchy J. 1987. Constitutional karyotypes in retinoblastoma. *Ophthalmic Paediatr Genet* 8:11–17.
- Velagaleti GV, Bien-Willner GA, Northup JK, Lockhart LH, Hawkins JC, Jalal SM, Withers M, Lupski JR, Stankiewicz P. 2005. Position effects due to chromosome breakpoints that map approximately 900 Kb upstream and approximately 1.3 Mb downstream of SOX9 in two patients with campomelic dysplasia. *Am J Hum Genet* 76:652–662.
- Vissers LE, van Ravenswaaij CM, Admiraal R, Hurst JA, De Vries BB, Janssen IM, van der Vliet WA, Huys EH, de Jong PJ, Hamel BC, Schoenmakers EF, Brunner HG, Veltman JA, van Kessel AG. 2004. Mutations in a new member of the chromodomain gene family cause CHARGE syndrome. *Nat Genet* 36:955–957.
- Wall JS, Paulus MJ, Gleason S, Gregor J, Solomon A, Kennel SJ. 2006. Micro-imaging of amyloid in mice. *Methods Enzymol* 412:161–182.
- Wallace MR, Marchuk DA, Andersen LB, Letcher R, Odeh HM, Saulino AM, Fountain JW, Brereton A, Nicholson J, Mitchell AL. 1990. Type 1 neurofibromatosis gene: Identification of a large transcript disrupted in three NF1 patients. *Science* 249: 181–186.
- Whiteford ML, Baird C, Kinmond S, Donaldson B, Davidson HR. 2000. A child with bisatellited, dicentric chromosome 15 arising from a maternal paracentric inversion of chromosome 15q. *J Med Genet* 37:E11.
- Wilson GN, Sauder SE, Bush M, Beitins IZ. 1985. Phenotypic delineation of ring chromosome 15 and Russell-Silver syndromes. *J Med Genet* 22:233–236.
- Woodage T, Basrai MA, Baxevanis AD, Hieter P, Collins FS. 1997. Characterization of the CHD family of proteins. *Proc Natl Acad Sci USA* 94:11472–11477.
- You LR, Takamoto N, Yu CT, Tanaka T, Kodama T, Demayo FJ, Tsai SY, Tsai MJ. 2005. Mouse lacking *COUP-TFII* as an animal model of Bochdalek-type congenital diaphragmatic hernia. *Proc Natl Acad Sci USA* 102:16351–16356.
- Zemni R, Bienvenu T, Vinet MC, Sefiani A, Carrie A, Billuart P, McDonnell N, Couvert P, Francis F, Chafey P, Fauchereau F, Friocourt G, Portes V, Cardona A, Frints S, Meindl A, Brandau O, Ronce N, Moraine C, Bokhoven H, Ropers HH, Sudbrak R, Kahn A, Fryns JP, Beldjord C. 2000. A new gene involved in X-linked mental retardation identified by analysis of an X;2 balanced translocation. *Nat Genet* 24:167–170.
- Zhang Y, LeRoy G, Seelig HP, Lane WS, Reinberg D. 1998. The dermatomyositis-specific autoantigen Mi2 is a component of a complex containing histone deacetylase and nucleosome remodeling activities. *Cell* 95:279–289.